Sustained dynamics of a weakly excitable system with nonlocal interactions

Yasuaki Kobayashi,[1,*] Hiroyuki Kitahata,[2] and Masaharu Nagayama[3,4]
[1]*Center for Simulation Sciences, Ochanomizu University, Tokyo 112-8620, Japan*
[2]*Department of Physics, Chiba University, Chiba 263-8522, Japan*
[3]*Research Institute for Electronic Science, Hokkaido University, Sapporo 060-0812, Japan*
[4]*JST CREST, Saitama 332-0012, Japan*
(Received 4 May 2017; published 23 August 2017)

We investigate a two-dimensional spatially extended system that has a weak sense of excitability, where an excitation wave has a uniform profile and propagates only within a finite range. Using a cellular automaton model of such a weakly excitable system, we show that three kinds of sustained dynamics emerge when nonlocal spatial interactions are provided, where a chain of local wave propagation and nonlocal activation forms an elementary oscillatory cycle. Transition between different oscillation regimes can be understood as different ways of interactions among these cycles. Analytical expressions are given for the oscillation probability near the onset of oscillations.

DOI: 10.1103/PhysRevE.96.022213

I. INTRODUCTION

Emergence of sustained dynamics from elements whose dynamics themselves are not oscillatory is a common phenomenon. Network connections of nonoscillatory elements, for instance, give rise to such dynamics and have been studied in various contexts, including gene networks [1], epidemic spreading dynamics [2–5], and generic excitable units [6–10],

Excitable units undergo oscillations in many ways: Simple two excitable systems can exhibit sustained dynamics when delay-coupled [11]; spatially extended excitable media can produce sustained spiral waves by introducing a perturbation leading to the formation of a spiral core [12]; one can even consider interactions at a distance through nonlocal links embedded in spatially extended systems [13–16], which eventually forms network structures composed of wave propagation and nonlocal interactions.

Waves in excitable media usually have an infinite propagation range, but we occasionally encounter systems that have a weaker sense of excitability. An example is found in calcium propagation in the epidermis [17], where waves of calcium excitation in epidermal cells have a finite propagation range as opposed to normal excitable waves. Also the wave profile is uniform rather than pulselike, which is different from the cases of propagation failure [18,19]. Interestingly, such a localized wave can trigger secondary waves at distant places through backfiring of nerve signals, a phenomenon called axon reflex [20], which can be regarded as long-range connections.

This observation motivates us to investigate possible dynamics of weakly excitable media when network-connected excitable units are embedded in it. In this paper, we introduce a generic cellular automaton model of weak excitability characterized by a uniform wave profile and a finite propagation range and investigate a possibility of sustained dynamics when long-range connections are given. We show that there are three oscillatory regimes with distinct dynamical properties, depending on the ranges of wave interactions and the density of nonlocal links. These different oscillation regimes are understood as a result of emergence and interactions of oscillatory cycles, which are closed chains of local excitation waves and nonlocal links. In particular, the onset of oscillatory dynamics can be fully determined by the emergence probability of such cycles, which can be analytically treated.

This paper is organized as follows. In Sec. II we present our model. In Sec. III, we exemplify sustained dynamics and consider a minimal requirement for them. In Sec. IV we investigate dynamical behavior of our model for a wide range of parameters, where the three oscillation regimes are shown. Analytical results are given in Sec. V, where the oscillation probability is calculated in the regime of simple periodic oscillations, and the mechanism of the transition into different regimes are discussed. Difference and similarity compared to previous works are discussed, and possible applications are mentioned in Sec. VI.

II. THE MODEL

We consider a two-dimensional (2D) square lattice of $N \times N$ cells with periodic boundaries. Each cell i is assigned a nonnegative integer value $u_i(t)$, representing the activity of i at an integer time t. From these cells L pairs are chosen, for each of which a directed link is assigned from one cell (*sender node*) to the other (*receiver node*). For simplicity we require that a sender and a receiver for a given link are different, and that once a cell is chosen as a sender or a receiver for one link, it is not chosen any more for other links.

Each time step consists of two distinct excitation processes: local wave propagation and nonlocal activation. A local wave propagation process updates $u_i(t)$ to an intermediate state $\tilde{u}_i(t)$ as follows:

$$\tilde{u}_i(t) = \max_{j \in \mathcal{N}_i} \{u_j(t), u_i(t), 1\} - 1, \tag{1}$$

where $\mathcal{N}_i$ represents the neighboring cells of i. In this process, all cells decrease their activity by one, and then its value is replaced by the highest activity in $\mathcal{N}_i$.

Then a nonlocal activation process follows. Consider a link-connected sender node j and its receiver node k. The receiver node is activated when both the sender node and the receiver

*kobayashi.yasuaki@ocha.ac.jp

node satisfy activation conditions: For the sender node j, this condition is given by

$$\tilde{u}_j(t) > \max\{u_j(t), u_{\rm th}\}, \tag{2}$$

where $u_{\rm th}$ is a threshold, and for the receiver node k,

$$\tilde{u}_k(t) = 0. \tag{3}$$

The state at $t+1$ is finally determined as follows:

$$u_i(t+1) = \begin{cases} u_M & \text{if } i \text{ is an activated receiver node,} \\ \tilde{u}_i(t) & \text{else,} \end{cases} \tag{4}$$

where u_M is the maximum activity obtained by the activated node. In this setup, the cells containing receiver nodes are considered as ordinary excitable units: they eventually have refractory period and are able to get maximally excited. All the other cells, which have no refractory period, act as media for local wave propagation.

The two parameters u_M and $u_{\rm th}$ determine two effective spatial ranges of local wave propagation. Suppose that all cells are in the rest state ($u_i = 0$). Equation (1) means that, when a receiver node is activated at $t = 0$ and a wave is initiated, after t steps the wave propagates up to distance t, with all cells within its propagation range having the same activity value $u_M - t$. This wave can induce nonlocal activations through sender nodes that are within its propagation range t only when $u_M - t \geqslant u_{\rm th}$, or $t \leqslant u_M - u_{\rm th}$, due to Eq. (2). Hence, the *activation* range of the wave is defined as $u_M - u_{\rm th}$.

On the other hand, Eq. (3) implies that receiver nodes that are within the propagation range of the wave are hindered from getting activation from other sender nodes. Since the wave propagates up to distance u_M, and it takes u_M time steps for the wave to lose the ability to suppress their activation, the *suppression* range of the wave is u_M and the refractory time of an activated receiver node is also u_M [21].

For later use, we introduce a parameter $\rho := u_{\rm th}/u_M$. Since $u_M - u_{\rm th} = (1-\rho)u_M$, $1-\rho$ represents the relative activation range, i.e., the ratio of the activation range to the suppression range. Throughout this work the system size is set to $N = 200$. Hence, the model is fully specified by a parameter set $\{u_M, \rho, L\}$ and a way of distributing L links among the cells.

III. EXAMPLES OF SUSTAINED DYNAMICS

This system can exhibit sustained dynamics when nonlocal links are randomly provided. Figure 1(a) is such an example, where $L = 100$ nonlocal links are randomly given, with $u_M = 80$ and $\rho = 0$, and one chosen receiver node i is initially perturbed so that $u_i = u_M$, with all other cells set to zero. Note that our discrete system results in a square-shaped wave pattern: the distance between the two cells at (i,j) and (k,l) is given by $|i-k| + |j-l|$, and thus the equidistant wave front forms a square. Also note that the cells inside the wave front have the same activity. In 2D continuous systems this would be a disk-shaped wave pattern propagating within a finite distance, which has been observed in calcium dynamics of epidermis and also theoretically investigated [22].

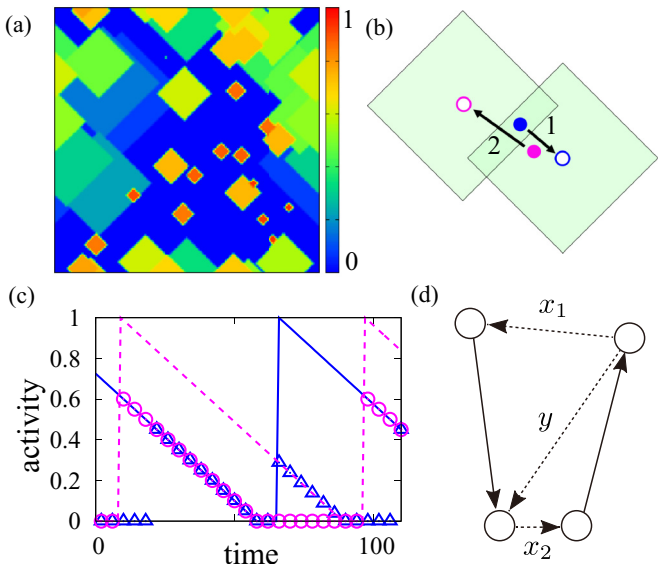

FIG. 1. (a) Snapshot of sustained dynamics in our model with $u_M = 50$, $\rho = 0$, and $L = 100$, where nonlocal links are randomly distributed. An initial perturbation is given to a chosen receiver node i as $u_i = u_M$, with all other cells are set to zero. The color bar indicates the activity of each cell relative to the maximum value u_M. (b) Example of a two-link oscillatory cycle. Arrows 1 and 2 represent directed nonlocal links from the sender node to the receiver node. Shaded square regions represent the activation range of local excitation waves from the receiver nodes, determined by $(1-\rho)u_M$. Coordinates of nodes: (104,114)→(158,68) (link 1, blue) and (121,78)→(27,140) (link 2, magenta). (c) Periodic oscillations observed in the two-link cycles described in (b), with $u_M = 80$, $\rho = 0$, and $L = 2$. Solid line: receiver node of link 1; triangles: sender node of link 1; broken line: receiver node of link 2; circles: sender node of link 2. (d) Diagram of a minimal oscillatory cycle. Solid arrows represent directed links; dotted arrows represent possible interactions through propagation of excitable waves; x_1 and x_2 represent the distance between the sender node of one link and the receiver node of the other, and y represents the distance between the two receiver nodes.

A. A single nonlocal link

What is the minimal requirement for sustained dynamics in this model? Let us first consider a system that contains only one nonlocal link whose sender node is within the activation range of its own receiver node. It is easy to confirm that sustained dynamics cannot be maintained by a single link: Suppose that the receiver node gets activated by perturbation and a local wave starts to propagate. While the local wave exists, the receiver node has nonzero activity and thus Eq. (3) is not satisfied; when the local wave disappears, Eq. (2) is no longer satisfied. Hence, nontrivial dynamical behavior requires more than one nonlocal link.

B. Two nonlocal links

The simplest case of sustained dynamics in this system is given by two links placed as in Fig. 1(b). Here the sender node of each link is influenced by a local wave generated from the

receiver node of the other link to form a cycle, whose dynamics is shown in Fig. 1(c).

Let x_1 (x_2) be the distance between receiver node 1 (receiver node 2) and sender node 2 (receiver node 1), and let y be the distance between the two receiver nodes, as depicted in Fig. 1(d). In order for two links to form an oscillatory cycle, the sender node of each link must be within the activation range of the receiver node of the other link, which is expressed as

$$x_1 < (1-\rho)u_M \quad \text{and} \quad x_2 < (1-\rho)u_M. \tag{5}$$

Also, the total signaling path must be sufficiently long so that the receiver nodes have time to recover from the refractory state:

$$x_1 + x_2 \geqslant u_M. \tag{6}$$

In addition, the two receiver nodes must be sufficiently separated, because otherwise a receiver node is suppressed by a local propagation wave from the other receiver node before it receives nonlocal activation. Let us call this *diagonal suppression*. The condition for the diagonal suppression not to occur is given by

$$y > x_1 \quad \text{and} \quad y > x_2. \tag{7}$$

Note that there is no condition required for the distance between the two sender nodes.

Equations (5), (6), and (7) are the necessary and sufficient conditions for a two-link cycle to exhibit oscillations. The range of the oscillation period T, which is equal to the total signaling path $x_1 + x_2$, is also determined by these conditions as

$$u_M \leqslant T < 2(1-\rho)u_M. \tag{8}$$

This means that the range of oscillation period vanishes when

$$\rho \geqslant \tfrac{1}{2}. \tag{9}$$

Therefore, two-cycle oscillatory cycles are impossible when the relative activation range is too short.

IV. DYNAMICAL PROPERTIES OF LINK DISTRIBUTION ENSEMBLES

Here we investigate what kind of dynamics is typically observed for a given parameter set $\{u_M, \rho, L\}$, when different distribution patterns of nonlocal links and different initial conditions are provided.

For a given parameter set $\{u_M, \rho, L\}$, $K(=1000)$ different samples are prepared, in each of which L links are randomly distributed under the condition that no single cell is assigned more than one nodes. For each sample we run simulations with different initial conditions: For each run, one chosen receiver node i is set to $u_i(0) = u_M$ and all other cells are set to zero. Since there are L receiver nodes, each sample has L possible initial conditions. Hence, each parameter set contains KL simulation runs.

Below, the parameter u_M is changed from $u_M = 10$ by 10 up to $u_M = 100$; and $u_{\rm th}$ values are chosen so that ρ changes by 0.1 from 0 to 0.8. Note that possible values of ρ is limited because both u_M and $u_{\rm th}$ are integers. All data in Fig. 2 are plotted using linear midpoint interpolation.

A. Oscillation probability

We define the oscillation probability of a given parameter set $\{u_M, \rho, L\}$ as follows. For each simulation run with the initial condition described above, we check if after $t_{\max}(=10\,000)$ time steps there are sustained dynamics, namely if $S := \sum_{i\in O} u_i(t_{\max}) > 0$, where O represents receiver nodes. Note that if $\sum_{i\in O} u_i(t) = 0$ at some $t = t^*$, then there is no further dynamics: $u_i(t) = 0$ for $\forall i$ and $t > t^*$. If, repeating this procedure for all L initial conditions, there is at least one initial condition that satisfies $S > 0$, the sample is judged to be oscillatory. Finally, the oscillation probability of a given parameter set is defined as the proportion of oscillatory samples to all K samples.

Figure 2(a) shows the oscillation probability as a function of u_M and ρ, with $L = 100$. For a fixed ρ value, the oscillation probability first increases as u_M increases and then decreases, and the oscillatory region becomes narrow as ρ increases.

Sustained dynamics can be periodic oscillations or complex oscillations; the latter case can be multiperiodic oscillations, chaotic oscillations, or long transient dynamics, but in this work we do not distinguish them. Figure 2(b) shows the probability of periodic oscillations. Here we can discern two band regions with high probabilities forming an inverted λ shape.

Comparing Figs. 2(a) and 2(b), we see that the low probability region of Fig. 2(a) are accounted for by the left and the right bands of λ, and thus can be explained by periodic oscillations, while the inner region with high oscillation probabilities mainly exhibit complex dynamics. The region of complex dynamics partly overlaps with the two band regions: Depending on different samples or different initial conditions, the same set of parameters can exhibit both periodic oscillations and complex dynamics.

This suggests that the oscillatory region can be divided into three regions, namely the left band region, the right band region, and the inner region between the two bands, each of which shows distinct dynamics indicated by statistical properties as shown below.

B. Active nodes

We define *active nodes* as those whose activities last at $t = t_{\max}$. More precisely, we call cell i active if $\sum_{t=t_{\max}/2}^{t_{\max}} u_i(t) \neq 0$. The active nodes are further classified into two: If an active node induces sustained dynamics of the whole system when chosen as an initial condition, we call it a *master node*; otherwise, we call it a *slave node*. Note that there can be nonactive nodes that can still induce sustained dynamics of the whole system. Such nodes are not counted as master nodes.

Difference between master and slave nodes will be illuminated when we consider an effective network consisting of local waves and nonlocal activations that are relevant to sustained dynamics. By definition, slave nodes in this network have only incoming links: In other words, slave nodes are passive player in this sustained dynamics. On the other hand, master nodes have both incoming links and outgoing links in this effective network. Note that those which have only outgoing links are the nodes which can induce sustained dynamics yet still are itself nonactive nodes. Dynamics induced by such nodes can also be induced by

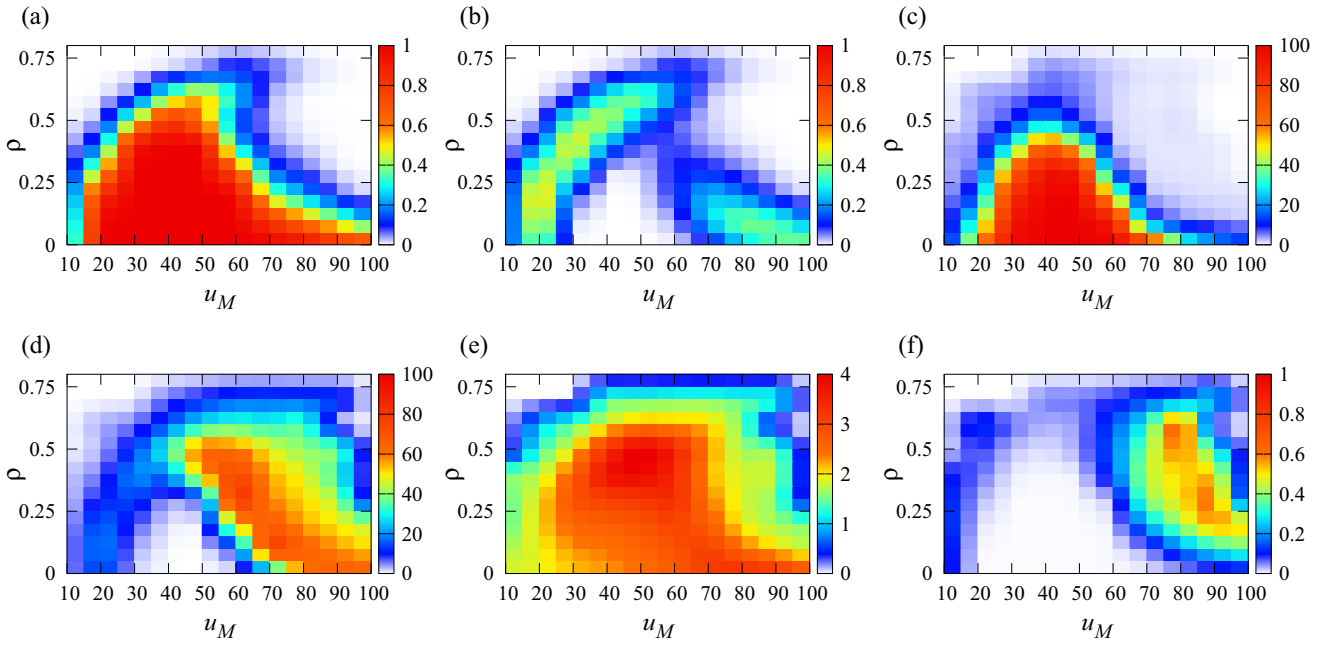

FIG. 2. Phase diagram of sustained dynamics with $L = 100$ nonlocal links in the parameter space of u_M and $\rho = u_{\rm th}/u_M$. (a) Oscillation probability defined as the proportion of oscillatory samples of randomly distributed L links to all samples. (b) Probability of periodic oscillations. (c) Number of master nodes. (d) Number of slave nodes. (e) Oscillation periods $T_{\rm per}$ for active nodes, normalized by the refractory time u_M. (f) Degree of synchronization σ for active nodes. In (c), (d), (e), and (f), values are averaged over all link distribution samples and all initial conditions with which sustained oscillations are observed.

directly perturbing the target nodes of these nodes, and our definition of master nodes exclude such nodes. Thus, master nodes defined in this way can be considered as organizing centers, and the sum of master and slave nodes (namely the total active nodes) determine the size of the sustained dynamics.

Figures 2(c) and 2(d) show these two types of active nodes, averaged over ensembles of all samples and initial conditions that show oscillatory dynamics. The two band regions have small number of master nodes, while the inner regions have many master nodes. Slave nodes are scarce in the inner region and rich in the right band region. In the left band region the total number of active nodes is small.

C. Oscillation period and coherence

Let $\mathcal{A}$ be the set of active nodes and $\mathcal{T}_i$ the set of all time moments when an active node i gets nonlocally activated in the time range $[t_{\max}/2, t_{\max}]$. Then the oscillation period $T_{\rm per}^{(i)}$ of receiver node i is defined as the average of time intervals in $\mathcal{T}_i$, and the oscillation period of the whole system $T_{\rm per}$ is defined as the average of $T_{\rm per}^{(i)}$ over $\mathcal{A}$.

Using these quantities, the degree of synchronization σ for the activity of the active nodes is defined as

$$\sigma = \left| \frac{1}{Z} \sum_{i \in \mathcal{A}} \sum_{t \in \mathcal{T}_i} \exp\left(\frac{2\pi i t}{T_{\rm per}} \right) \right|, \tag{10}$$

where $Z := \sum_{i \in \mathcal{A}} \sum_{t \in \mathcal{T}_i} 1$ is a normalization constant. The average $\langle \sigma \rangle$ for a given parameter set is calculated over all samples and initial conditions that show oscillatory dynamics; if there is no oscillatory sample, this value is set to zero. The average period $\langle T_{\rm per} \rangle$ is calculated in the same manner.

Figure 2(e) shows the average oscillation period normalized by the refractory time u_M. The observed period falls within the range $[u_M, 4u_M]$, and it tends to be large when the oscillation probability is large, indicating that this region tends to form longer and more complex cycles of active nodes. Indeed, since the period of two-link cycles is less than $2(1-\rho)u_M$ according to Eq. (8), cycles with more than two links must be involved in oscillations in the long-period region.

Figure 2(f) shows the degree of synchronization. The two band regions have nonzero $\langle \sigma \rangle$ values, while the most part of the inner region has vanishingly small values. The higher values in the right region indicates that oscillations are more coherent there. There is a region above the right band where $\langle \sigma \rangle$ is particularly high, although the oscillation probability itself is quite small there. It is also noticeable that $\langle \sigma \rangle$ values inversely correlate with the number of master nodes and that the high $\langle \sigma \rangle$ region partially overlaps with high-slave node region, indicating that synchronization is observed when a small number of active nodes dominate the entire system.

D. Three oscillation regimes

From the above observations, we can clearly discern three regions with different dynamical properties, as shown in Fig. 3.

In the left band region, the oscillation probability is relatively small, and the observed dynamics are mainly periodic [Fig. 3(a)]. Here small number of active nodes are involved, and the total activity of active receiver nodes are only slightly coherent, and this slight coherence can be explained by a small number of unevenly distributed signals. Therefore, it

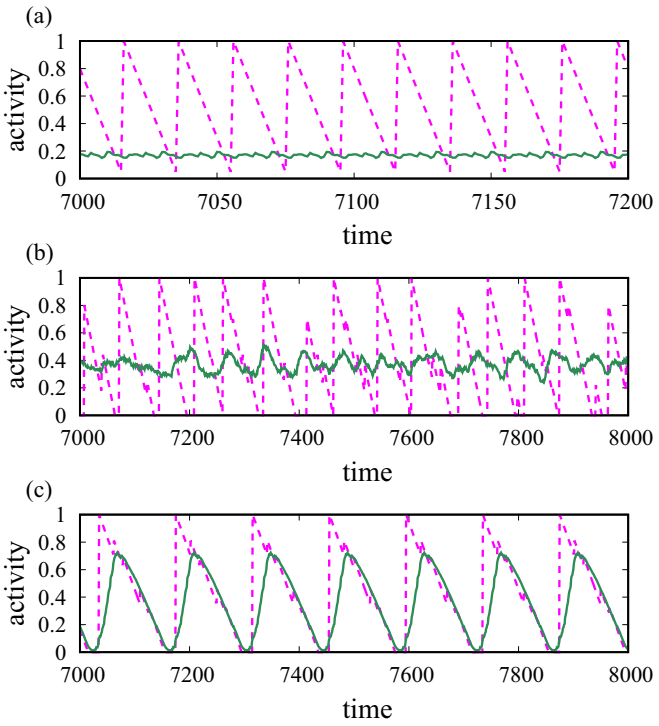

FIG. 3. Three typical examples of sustained dynamics for $L = 100$ contained in the phase diagram of Fig. 2: Broken lines represent the activity of a selected active node, and solid lines represent the average over all active nodes. (a) Incoherent periodic oscillations: $u_M = 20$, $\rho = 0.2$; (b) complex oscillations: $u_M = 50$, $\rho = 0$; (c) coherent periodic oscillations: $u_M = 90$, $\rho = 0.2$.

is expected that in this region a small number of oscillatory cycles are formed and their dynamics are independent of each other.

In the right band region, which is also characterized by periodic oscillations with small probabilities, a few master nodes govern many slave nodes and the resulting activity is more coherent [Fig. 3(c)], suggesting the existence of a small number of interacting oscillatory cycles.

The inner region has high oscillation probability, the observed dynamics being complex with longer periods and incoherent activities [Fig. 3(b)], which, together with the fact that most of the active nodes are master nodes, indicates that dynamics are generated by many interdependent active nodes. Note that the large-u_M side of this region is characterized by the existence of long transient times even when sustained oscillations are not observed (data not shown), another indication that many active nodes interact with each other. Also it should be noted that the region of the complex dynamics overlaps with both the left and the right bands.

Hence, what we typically observe in a statistical sense as increasing u_M for fixed ρ is a transition from incoherent periodic oscillations through complex oscillations to synchronized periodic oscillations. The same transition pattern is found when L increases for a certain range of ρ: Since the total oscillation probability has a unimodal shape [Fig. 2(a)], we can define an oscillation boundary inside which the oscillation probability is higher than a certain value $p^*(=0.2)$.

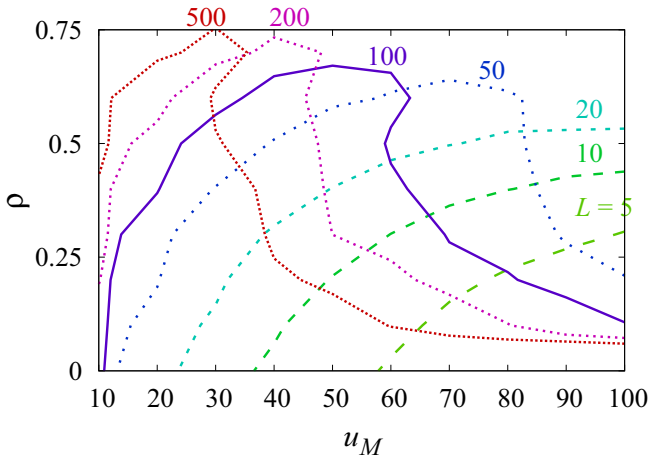

FIG. 4. Oscillation boundaries defined as the contour of the oscillation probability equal to 0.2, for different L values indicated adjacent to each curve. The curve for $L = 100$ corresponds to data in Fig. 2(a), and all other curves are calculated by performing the same numerical simulations as in Fig. 2(a) with different L values.

As shown in Fig. 4, the oscillation boundary shifts in the small-u_M direction as L increases, with the inverted λ structure maintained for large L values.

V. CALCULATION OF OSCILLATION PROBABILITY

As observed above, incoherent periodic oscillations are typically observed in the small-u_M region for a fixed ρ, and oscillatory cycles are expected to behave independently. In such cases the oscillation probability can be analytically treated. Below, first we calculate the oscillation probability of individual oscillatory cycles and then consider the oscillation probability of the whole system.

A. The two-link cycle

Let us rescale the length scale by the system size N so that the system is now $[0,1] \times [0,1]$. For large N, the distance can be treated as continuous, and a normalized parameter $z := u_M/N$ can also be treated as continuous. To make the following analysis easier, we restrict the range of the parameter u_M within $0 \leqslant u_M \leqslant N/2$, or equivalently z within $0 \leqslant z \leqslant 1/2$. Since we have assumed that links are distributed at random, the probability density $D(r)$ of the distance r between two randomly picked up nodes are given by

$$D(r) = \begin{cases} 4r & r < \frac{1}{2}, \\ 4(1-r) & r \geqslant \frac{1}{2}. \end{cases} \tag{11}$$

Here the periodic boundaries are taken into account.

Suppose that there are only two links in the system. The probability that the two links exhibit oscillations, denoted by $p^{(2)}$, is obtained as the probability that the distances of the two nodes fall into the area determined by Eqs. (5), (6), and (7):

$$p^{(2)}(z,\rho) = \int_{\Omega^{(2)}} dz_1 dz_2 dw\, D(z_1) D(z_2) D(w), \tag{12}$$

where $\Omega^{(2)}$ is determined by Eqs. (5), (6), and (7), rewritten in terms of normalized distances $z_1 := x_1/N$, $z_2 := x_2/N$, and $w := y/N$. Performing the integration, we obtain

$$p^{(2)}(z,\rho) = a(\rho)z^4 - b(\rho)z^6, \tag{13}$$

where

$$a(\rho) = \frac{2(1-2\rho)^2(5-4\rho)}{3}, \tag{14}$$

$$b(\rho) = \frac{(1-2\rho)^2(49-124\rho+108\rho^2-32\rho^3)}{10}, \tag{15}$$

which are positive for $0 \leqslant \rho < \frac{1}{2}$ and vanish at $\rho = \frac{1}{2}$. Since $0 < z < \frac{1}{2}$, the second term of Eq. (13), which corresponds to the diagonal suppression, is a higher order correction that decreases the oscillation probability.

B. The *n*-link cycle

Now let us consider n links arranged in an cyclic order. It becomes a complicated task to compute the oscillation probability of the n-link cycle $p^{(n)}(z,\rho)$. Here we focus only on the lowest order of z for each n, which is obtained by neglecting diagonal suppression.

An oscillatory n-link cycle can be obtained when (normalized) distances between a receiver node of one link and the sender node of the next link, denoted by z_i $(i = 1,\ldots,n)$, satisfy the following conditions:

$$z_i < (1-\rho)z \quad \text{for } \forall i = 1,\cdots,n, \tag{16}$$

and

$$z_1 + \cdots + z_n \geqslant z. \tag{17}$$

This is a generalization of the condition for the two-link cycle with diagonal suppressions neglected. From this it follows that the n-link cycle has a nonzero oscillation probability only if

$$\rho < \frac{n-1}{n}. \tag{18}$$

Thus, even when 2-cycles ceases to oscillate at $\rho = 1/2$, larger cycles with $n > 2$ can still be oscillatory, which accounts for nonzero probabilities found in the region of $\rho > 1/2$ in Fig. 2(a).

The lowest-order oscillation probability $p_0^{(n)}(z,\rho)$ is then given by

$$\begin{aligned} p_0^{(n)}(z,\rho) &= \int_{\Omega_0^{(n)}} dz_1 \cdots dz_n D(z_1)\cdots D(z_n) \\ &= a_n(\rho)z^{2n}, \end{aligned} \tag{19}$$

where $\Omega_0^{(n)}$ is the region defined by Eqs. (16) and (17). Although it is difficult to obtain analytical expression of $a_n(\rho)$ for general ρ, the integration can be performed when $\rho < 1/2$, which yields

$$\begin{aligned} a_n(\rho) &= 2^n(1-\rho)^{2n} \\ &\quad - \frac{4^n}{(2n)!}\{1 - n[2n-(2n-1)\rho]\rho^{2n-1}\}. \end{aligned} \tag{20}$$

As in the case of $n = 2$, neglecting diagonal suppressions implies the overestimation of the oscillation probability. Roughly speaking, each local connection in a cycle contributes to the overall oscillation probability by a factor of $O(z^2)$, while each diagonal suppression contributes to it by $1 - O(z^2)$. Therefore, the oscillation probability is given at the lowest order by $O(z^{2n})$, and the diagonal suppression can be treated as a higher-order correction of order $O(z^{2n+2})$.

C. Oscillation probability of the whole system with *L* nonlocal links

Now consider the oscillation probability of the whole system when L links are randomly provided. Under the present assumption that individual oscillatory cycles behave independently, the whole system is oscillatory if at least one oscillatory cycle of size $n \geqslant 2$ is formed. Considering that the probability of n-cycle oscillations is $O(z^{2n})$, one might be tempted to think that the contribution from large cycles are neglected. However, such large cycles cannot be neglected in the case of large L because of a large number of possible combinations of links to form cycles: Since there are $c(L,m) = (m-1)!\binom{L}{m}$ ways of forming m-cycles from L links, the oscillation probability of the whole system, denoted by $p_L^{\mathrm{tot}}(z,\rho)$, is written as

$$p_L^{\mathrm{tot}}(z,\rho) = 1 - \prod_{m=2}^{L}[1 - p^{(m)}(z,\rho)]^{c(L,m)}. \tag{21}$$

Figure 5(a) shows oscillation probability as a function of $z = u_M/N$ for different L values with $\rho = 0$, where theoretical curves are given by Eq. (21) with $p^{(m)}$ approximated by $p_0^{(m)}$ [Eqs. (19) and (20)] except for $m = 2$. For small u_M they show good agreement with numerical data. In particular, better agreement is achieved for larger L. We have numerically confirmed that in Eq. (21) cycles with $m \leqslant 4$ make nonnegligible contributions to the overall oscillation probability for large L.

For small z, $p_L^{\mathrm{tot}}(z,\rho)$ is approximated by

$$p_L^{\mathrm{tot}}(z,\rho) = \sum_{m=2}^{L} c(L,m)p^{(m)}(z,\rho). \tag{22}$$

In particular, for large L, there exists a range of z such that only the first several terms satisfying $m \ll L$ contribute to the sum. In this case the approximation $c(L,m)p^{(m)} \approx (L^m/m)a_m(\rho)z^{2m}$ is justified and the L-dependence of the upper bound of the summation can be neglected. This means that p_L^{tot} can be expressed using some function ϕ as

$$p_L^{\mathrm{tot}}(z,\rho) = \phi(L^{1/2}z,\rho). \tag{23}$$

Although this relationship holds only for small z, the scaling itself is valid for a wider range: For a given ρ value, numerical data with different values of L from $L = 10$ to $L = 1000$ accumulates on the same theoretical curve of $p_L^{\mathrm{tot}}(z,\rho)$ when plotted as a function of $L^{1/2}z$, as shown in Fig. 5(b). This scaling implies that sustained dynamics of the system can be expected when $L^{1/2}z = O(1)$, or $u_M^2/N^2 = O(1/L)$, which can be interpreted as the probability of finding at least one link in the vicinity of the effective range of one node, whose area is approximately $O(u_M^2)$.

There are two reasons for deviation of numerical data from the theoretical curves. One is the approximation ignoring

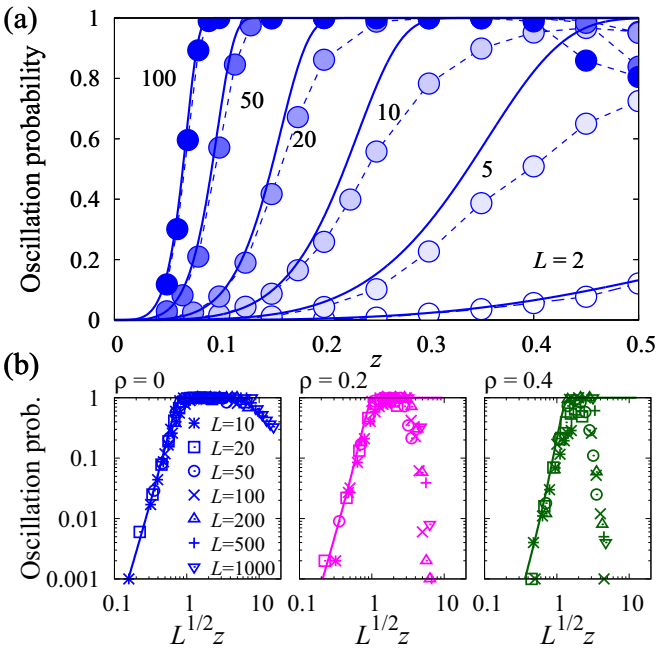

FIG. 5. (a) Oscillation probability as a function of $z = u_M/N$ for $\rho = 0$ with different L values. Circles are numerical data and solid curves are theoretical prediction given by $p_L^{\rm tot}(z,\rho)$. (b) Oscillation probability as a function of $L^{1/2}z$ for three different ρ values, for each of which data for different L values from $L = 10$ to $L = 1000$ are plotted. Solid curves are given by $p_L^{\rm tot}(z,\rho)$, where for each ρ value only one curve with $L = 1000$ is presented: For each ρ value, curves of $p_L^{\rm tot}(z,\rho)$ with different L values converge to one curve as $L \to \infty$ when plotted as a function of $L^{1/2}z$, and for $L \geqslant 10$ they are almost indistinguishable. For each parameter set, the oscillation probability is calculated in the same way as in Fig. 2(a).

diagonal suppressions, which accounts for underestimation of oscillation probabilities in Fig. 5(a). Since this correction becomes effective for large u_M, it does not affect the system with large L, where $p_L^{\rm tot}$ reaches unity for small u_M.

If z becomes large, or if L becomes large with fixed z, the decrease of the oscillation probability becomes prominent, as shown in Figs. 5(b) and 2(a). In these cases, it becomes likely that links consisting of one oscillatory cycle are also members of other cycles, and their interactions cannot be neglected.

D. Interference of cycles

If more than one oscillatory cycle are interfering with each other, the one with the shortest oscillation period survives, so that the sustained dynamics of the whole system persist. But an oscillatory cycle is not only affected by other oscillatory cycles: a different kind of cycle must also be taken into account, namely the cycles that satisfy the condition for local connections [Eq. (16)] but not the condition for the recovery from the refractory time [Eq. (17)]. When a receiver node of such cycles is activated, a chain of activation events circulates and stops at the first activated nodes. Such cycles can be called *excitable cycles*.

If a link in an oscillatory cycle is also a member of an excitable cycle, it is possible that excitable cycles suppress activation of the receiver node of that link. Therefore their

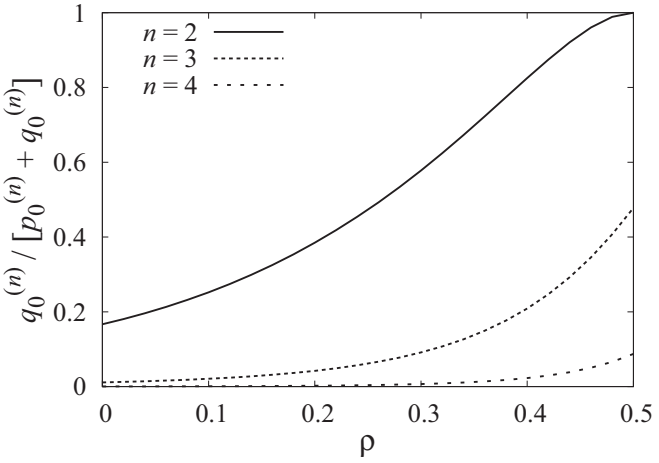

FIG. 6. Conditional probability of the formation of an excitable n-cycle when n links form either an oscillatory or an excitable cycle, given by $q_0^{(n)}/[p_0^{(n)} + q_0^{(n)}]$, for $n = 2$, 3, and 4.

interactions result in the decrease of the oscillation probability. Furthermore, if several oscillatory cycles are interacting as described above, suppression of the cycle with the shortest period among them by an excitable cycle may lead to reactivation of the second shortest oscillatory cycle previously hindered by the shortest one, and the resulting dynamics can be complex. This accounts for the observed complex oscillations in the middle range.

The condition for the formation of an excitable cycle is at the lowest order of z is given by Eq. (16) and

$$z_1 + \cdots + z_n < z. \tag{24}$$

Then the probability of having an excitable cycle with n links, denoted by $q_0^{(n)}$, is given by (again for $\rho < 1/2$)

$$\begin{aligned} q_0^{(n)} &= \int_0^{(1-\rho)z} dz_1 \cdots \int_0^{(1-\rho)z} dz_n D(z_1)\cdots D(z_n) - p_0^{(n)} \\ &= 2^n(1-\rho)^{2n} z^{2n} - p_0^{(n)}. \end{aligned} \tag{25}$$

Thus, as z increases, not only oscillatory cycles but excitable cycles tend to form. As shown in Fig. 6, when a cycle of size n is formed, the probability that it is not oscillatory but excitable becomes larger with smaller n and larger ρ. Also, since the number of possible link combinations increases as L, the number of excitable cycles also increases, and it is more and more difficult for oscillatory cycles to find a place that is outside of the suppression range of excitable cycles. These facts account for ρ dependence of the right side of the oscillation boundary and its leftward shift as the increase of L in Fig. 4.

Such interactions are also responsible for coherent oscillations with small probabilities. Since there are many interacting cycles in these cases, most of the space is covered with the suppression range of oscillatory and excitable cycles. As a result, either oscillation cannot survive or only a few master nodes with the same oscillation period survive, which can participate in coherent oscillations.

VI. DISCUSSIONS

In a model system with a uniform and finite-range excitation wave, we have found sustained oscillations generated by oscillatory cycles made of a closed chain of local waves and nonlocal activation links. Three distinct regions of sustained dynamics, namely incoherent periodic oscillations, complex oscillations, and coherent periodic oscillations, can be observed in this order when the wave range or the nonlocal link density is increased. This transition of dynamics is understood as the increased appearance of oscillatory cycles and then interactions among oscillatory and excitable cycles.

This model can be regarded as a simplified epidermal system: cell grids correspond to layers of epidermal cells, and sender and receiver nodes connected by a link correspond to branching tips of a nerve fiber embedded in the epidermal layers. In epidermis, the propagation range of calcium waves in epidermal cells depends on stimulation intensity, and sustained local excitations are also observed when strong stimulation is given [22]. On the other hand, the nerve fibers do behave as usual excitable systems. A sender end of a branched fiber gets stimulated by excited epidermal cells and sends a signal to the corresponding receiver end, where it releases some peptide that induce excitation of neighboring epidermal cells [20]. Hence, epidermal system is considered as a complex of network-connected excitable units and weakly excitable media with finite interaction ranges.

Since the local wave is uniform within its propagation range, all nodes covered with it are suppressed until it disappears. Therefore, in our model it would be both uninteresting and unrealistic to consider too large propagation ranges, while the cases of short propagation ranges might be responsible for sustained sensation observed in pathological epidermal systems [23], where the density of nerve fibers is not necessarily large but many branchings are found [24], which provide places for axon reflexes and thereby yield many nonlocal connections. Indeed, as a more realistic model of epidermal systems it is possible to construct a continuous version of the present model, incorporating a model of calcium propagation in the epidermis [22].

Our results can be compared to previous works of excitable systems with nonlocal interactions. First of all, our model does not reduce to an usual excitable system even when we set the wave propagation range equal to the system size, because the wave profile is different from a normal excitable wave. Nevertheless, similar transitions have been observed in these systems, namely from no dynamics through oscillations to disappearance of dynamics [14,15]. Our results suggest that long-range wave propagation is not a prerequisite for such dynamical behavior.

Dynamical behavior observed in this model can also be compared to oscillatory gene networks [25], where randomly connected genes usually show periodic oscillations with basic oscillatory cycles, while rare networks that are found by evolutionary engineering show multiperiodic, synchronous periodic, and chaotic oscillations, which can also be understood as interaction of oscillatory and excitable cycles.

ACKNOWLEDGMENT

This work was supported by JST CREST Grant No. JPMJCR15D2, Japan.

[1] M. B. Elowitz and S. Leibler, Nature **403**, 335 (2000).
[2] T. Gross and I. G. Kevrekidis, Europhys. Lett. **82**, 38004 (2008).
[3] X. Li and X. Wang, IEEE Trans. Autom. Control **51**, 534 (2006).
[4] Y. Hayashi, M. Minoura, and J. Matsukubo, Phys. Rev. E **69**, 016112 (2004).
[5] V. Agrawal, P. Moitra, and S. Sinha, Sci. Rep. **7**, 41582 (2017).
[6] X. Liao, Q. Xia, Y. Qian, L. Zhang, G. Hu, and Y. Mi, Phys. Rev. E **83**, 056204 (2011).
[7] A. Keane, T. Dahms, J. Lehnert, S. A. Suryanarayana, P. Hövel, and E. Schöll, Eur. Phys. J. B **85**, 407 (2012).
[8] P. McGraw and M. Menzinger, Phys. Rev. E **83**, 037102 (2011).
[9] Y. Qian, Phys. Rev. E **90**, 032807 (2014).
[10] J. Wang and Z. Liu, Europhys. Lett. **95**, 10001 (2011).
[11] M. A. Dahlem, G. Hiller, A. Panchuk, and E. Schöll, Int. J. Bifurcat. Chaos **19**, 745 (2009).
[12] E. Meron, Phys. Rep. **218**, 1 (1992).
[13] M. Tinsley, J. Cui, F. V. Chirila, A. Taylor, S. Zhong, and K. Showalter, Phys. Rev. Lett. **95**, 038306 (2005).
[14] A. J. Steele, M. Tinsley, and K. Showalter, Chaos **16**, 015110 (2006).
[15] S. Sinha, J. Saramäki, and K. Kaski, Phys. Rev. E **76**, 015101 (2007).
[16] Y. Qian, X. Huang, G. Hu, and X. Liao, Phys. Rev. E **81**, 036101 (2010).
[17] M. Tsutsumi, K. Inoue, S. Denda, K. Ikeyama, M. Goto, and M. Denda, Cell Tissue Res. **338**, 99 (2009).
[18] J. P. Keener, SIAM J. Appl. Math. **47**, 556 (1987).
[19] S. Kádár, J. Wang, and K. Showalter, Nature **391**, 770 (1998).
[20] Ö. Hägermark, T. Hökfelt, and B. Pernow, J. Invest. Dermatol. **71**, 233 (1978).
[21] One could think of different rules describing local propagation and nonlocal activation: For instance, self-activation of a single link is possible if we discard Eq. (3). Such a model can induce oscillations too easily and the resulting dynamical behavior would be trivial and uninteresting. Also, a simpler activation condition could be adopted for the sender nodes instead of Eq. (2), such as $\tilde{u}_i(t) > u_{\rm th}$. This rule would mean that the sender node keeps sending activation signals to the receiver node while its activity is higher than $u_{\rm th}$, and therefore it is easier to cause nonlocal activation. Indeed, we have numerically confirmed that this does not cause qualitative differences to the results of this paper, although more complicated calculation will be required if we try to obtain analytical results.
[22] Y. Kobayashi, Y. Sanno, A. Sakai, Y. Sawabu, M. Tsutsumi, M. Goto, H. Kitahata, S. Nakata, J. Kumamoto, M. Denda, and M. Nagayama, PLoS ONE **9**, e92650 (2014).
[23] S. R. Wilson, L. Thé, L. M. Batia, K. Beattie, G. E. Katibah, S. P. McClain, M. Pellegrino, D. M. Estandian, and D. M. Bautista, Cell **155**, 285 (2013).
[24] M. Tsutsumi, H. Kitahata, M. Fukuda, J. Kumamoto, M. Goto, S. Denda, K. Yamasaki, S. Aiba, M. Nagayama, and M. Denda, Br. J. Dermatol. **174**, 191 (2016).
[25] Y. Kobayashi, T. Shibata, Y. Kuramoto, and A. S. Mikhailov, Eur. Phys. J. B **76**, 167 (2010).